THE JOURNAL OF PHYSICAL CHEMISTRY C

Article

Cite This: J. Phys. Chem. C 2019, 123, 36−47

pubs.acs.org/JPCC

Tailoring Photophysical Processes of Perylene-Based Light Harvesting Antenna Systems with Molecular Structure and Solvent Polarity

Damla Inan,[†] Rajeev K. Dubey,[†,‡] Wolter F. Jager,[*,‡] and Ferdinand C. Grozema[*,†]

[†]Laboratory of Optoelectronic Materials and [‡]Laboratory of Organic Materials & Interfaces, Department of Chemical Engineering, Delft University of Technology, Van der Maasweg 9, 2629 HZ Delft, The Netherlands

Supporting Information

ABSTRACT: The excited-state dynamics of perylene-based bichromophoric light harvesting antenna systems has been tailored by systematic modification of the molecular structure and by using solvents of increasing polarity in the series toluene, chloroform, and benzonitrile. The antenna systems consist of blue light absorbing naphthalene monoimide (NMI) energy donors (**D1**, **D2**, and **D3**) and the perylene derived green light absorbing energy acceptor moieties, 1,7-perylene-3,4,9,10-tetracarboxylic tetrabutylester (**A1**), 1,7-perylene-3,4,9,10-tetracarboxylic monoimide dibutylester (**A2**), and 1,7-perylene-3,4,9,10-tetracarboxylic bisimide (**A3**). The design of these antenna systems is such that all exhibit ultrafast excitation energy transfer (EET) from the excited donor to the acceptor, due to the effective matching of optical properties of the constituent chromophores. At the same time, electron transfer from the donor to the excited acceptor unit has been limited by the use of a rigid and nonconjugated phenoxy bridge to link the donor and acceptor components. The antenna molecules **D1A1**, **D1A2**, and **D1A3**, which bear the least electron-rich energy donor, isopentylthio-substituted NMI **D1**, exhibited ultrafast EET (τ_{EET} ∼ 1 ps) but no charge transfer and, resultantly, emitted a strong yellow-orange acceptor fluorescence upon excitation of the donor. The other antenna molecules **D2A2**, **D2A3**, and **D3A3**, which bear electron-rich energy donors, the amino-substituted NMIs **D2** and **D3**, exhibited ultrafast energy transfer that was followed by a slower (ca. 20−2000 ps) electron transfer from the donor to the excited acceptor. This charge transfer quenched the acceptor fluorescence to an extent determined by molecular structure and solvent polarity. These antenna systems mimic the primary events occurring in the natural photosynthesis, i.e., energy capture, efficient energy funneling toward the central chromophore, and finally charge separation, and are suitable building blocks for achieving artificial photosynthesis, because of their robustness and favorable and tunable photophysical properties.

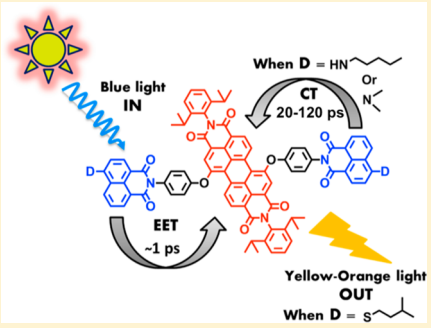

INTRODUCTION

Artificial light-harvesting antenna systems are key elements for an efficient solar energy conversion because of their ability to harvest a substantial part of the incident light.[1−4] Their structural and functional designs are often inspired by nature, most specifically from natural photosynthesis, in which efficient energy capture, efficient energy funneling to the reaction center, and charge separation occur in a sequential manner as primary events.[5−7] Artificial antenna systems are generally composed of an organized group of chromophores with distinct chemical structures and complementary absorption spectra to maximize the absorption of visible light.[4,8−10] An idealized light-harvesting antenna must enable efficient energy capture and efficient transfer of excitation energy among the constituent chromophores, so that the absorbed energy can be efficiently funneled to the reactive site.[10,11] In order to perform efficiently, the antenna systems also require a perfect match of electronic properties between constituent chromophores, so that competing photoinduced processes will be eliminated.

Photoinduced charge transfer is the major process that competes with energy transfer.[9,12−14] Therefore, limiting the rate of charge transfer is an important challenge in designing efficient artificial light harvesting antenna systems. Whether or not charge transfer processes take place primarily depends on the energy of the charge-separated state relative to the energies of singlet excited states of constituent chromophores. Since energies of charge-separated states are lower in polar environments, charge transfer becomes more feasible in polar solvents.[15] However, rates of charge transfer, apart from the thermodynamic driving force, also depend on kinetic factors which are influenced by the attachment of the donor chromophores to the acceptor. Consequently, the major challenges in designing such artificial antenna systems are to keep a good balance of spectral and electronic properties of the constituting chromophores and to choose an appropriate linking strategy with respect to the position and the identity of the linker units between the donors and the acceptor.

Received: August 31, 2018
Revised: December 18, 2018
Published: December 18, 2018

DOI: 10.1021/acs.jpcc.8b08503
J. Phys. Chem. C 2019, 123, 36−47

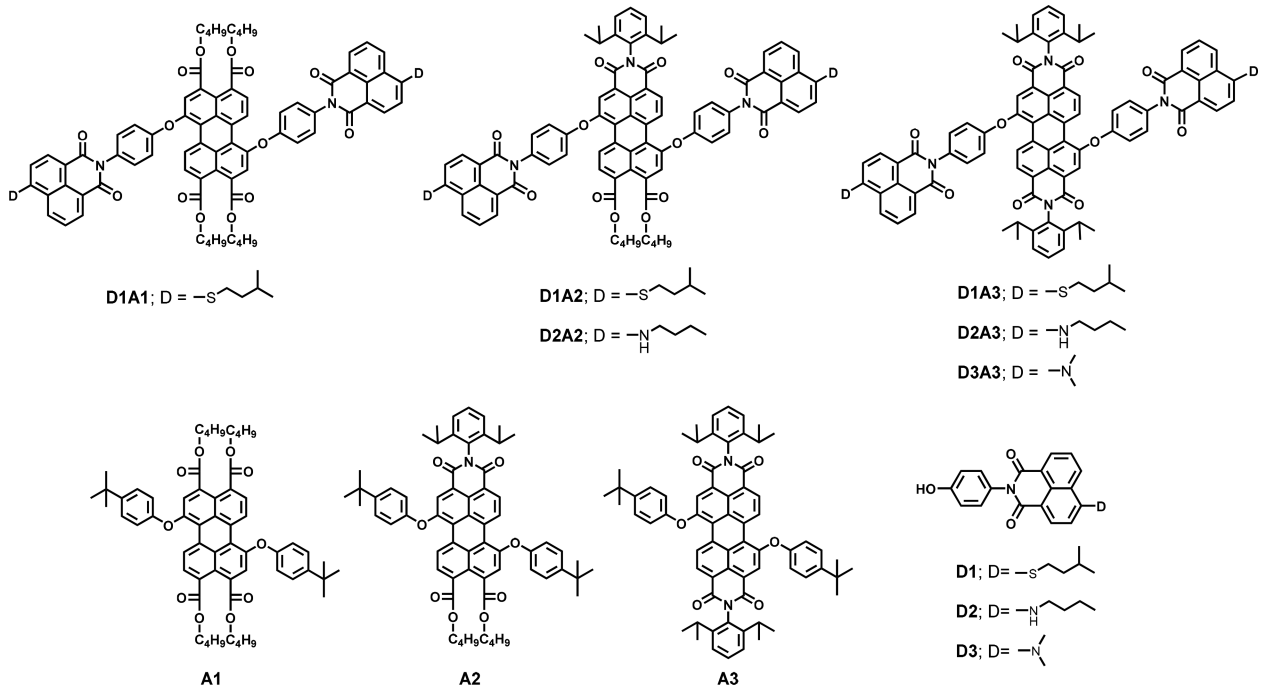

Figure 1. Chemical structures of the studied light-harvesting antennae based on perylene tetracarboxylic acid derivatives (**A1**, **A2**, and **A3**) and naphthalene monoimides (**D1**, **D2**, **D3**).

Among suitable chromophores for building light-harvesting antennae, perylene bisimides (PBIs) are particularly attractive, due to their high photochemical and thermal stability, ease of functionalization, strong absorption in the visible region of the solar spectrum, and almost negligible triplet yield.[16,17] Taking advantage of these favorable properties, PBIs have been widely used as the constituent chromophore in light-harvesting antenna systems.[9,12,18−24] However, due to the high electron deficiency of the PBI core, competing charge transfer has often been observed among constituent chromophores within these antenna systems, even if PBIs are covalently coupled with moderately electron-rich energy donors.[9,12−14,25,23,26]

Recently, we reported the modular design, synthesis, and photophysical characterization of five bichromophoric light-harvesting antennae, which were constructed by the covalent attachment of blue light absorbing naphthalene monoimide (NMI) energy donors to green light absorbing perylene tetracarboxylic acid (PTCA) derived energy acceptors.[27] In addition to the highly electron deficient PBI, we introduced the less electron deficient but highly stable perylene tetraester (PTE)[28] and perylene monoimide diester (PMIDE) as energy acceptors. We successfully demonstrated that these donor and acceptor molecules possess excellent spectral overlap between the donor's emission spectra and the acceptor's absorption spectra, which facilitates an efficient and ultrafast ($\tau_{EET} \sim 1$ ps) energy transfer via the FRET mechanism in the antenna molecules.[27] Simultaneously, intramolecular charge transfer was not observed, not even for PBI-based antenna systems where this process may be thermodynamically allowed. All of the reported results, however, were obtained in the apolar solvent toluene, which suppresses charge transfer processes.[29] In artificial photosynthesis, however, charge separation processes in the reaction center are a prerequisite for performing chemical reactions and therefore it is of paramount importance that these molecules are excellent antenna systems in polar solvents as well.

Herein, we report on the effect of molecular structure and solvent polarity on the excited-state dynamics of antenna systems composed of NMI energy donors and PTCA energy acceptors. We have investigated the six antenna molecules **D1A1**, **D1A2**, **D2A2**, **D1A3**, **D2A3**, and **D3A3** depicted in Figure 1 and selected the polar solvents chloroform and benzonitrile, to complement the results obtained previously in toluene.[29] Steady-state absorption and emission spectroscopy, time-dependent fluorescence measurements, and femtosecond pump−probe spectroscopy have been employed to investigate in detail the photophysical behavior of these antenna systems. Model donor (**D1**, **D2**, **D3**) and model acceptor (**A1**, **A2**, **A3**) compounds were also studied under the same experimental setup to characterize the excited states of the constituent chromophores (Figure 1). Electrochemical measurements were performed, and charge separation energies ΔG^0_{CS} were calculated in order to correlate the rates of photoinduced charge transfer with the energetics of this process. Finally, the structure−property relationships of the antenna molecules and their molecular design are discussed and evaluated in the framework of their application within artificial photosynthesis.

METHODS

Materials. All of the reagents utilized in the synthesis were purchased from commercial suppliers and used as received unless otherwise stated. Toluene was dried over sodium under an argon atmosphere prior to use. NMP, used for the reaction, was of anhydrous grade. Purification of the products was performed by column chromatography (silica gel 60, mesh size 0.063−0.200 mm). TLC plates and the sorbent for the column chromatography were purchased from commercial suppliers. All solvents used in the spectroscopic measurements were of reagent grade and were used as received from suppliers.

Instrumentation and Characterization. The NMR spectra were recorded with a 400 MHz pulsed Fourier transform NMR spectrometer in either $CDCl_3$ or DMSO-d_6

DOI: 10.1021/acs.jpcc.8b08503
J. Phys. Chem. C 2019, 123, 36−47

at room temperature. The chemical shift values are given in ppm and J values in Hz. High-resolution mass spectra were collected on an AccuTOF GC v 4g, JMS-T100GCV, mass spectrometer (JEOL, Japan). An FD/FI probe (FD/FI) equipped with an FD Emitter, Carbotec (Germany), FD 10 μm, was used. Typical measurement conditions were as follows: current rate 51.2 mA/min over 1.2 min; counter electrode −10 kV; ion source 37 V. The samples were prepared in dichloromethane.

The electrochemical behavior of the compounds was studied by cyclic voltammetry (CHI 600D electrochemical analyzer) in a three-electrode single-compartment cell consisting of a platinum electrode as the working electrode, a Ag wire as the reference electrode, and a Pt wire as the counter electrode (scan rate = 0.10 V/s). The cell was connected to the computer controlled potentiostat (CH Instruments Inc. 600D). Predried CH_2Cl_2 containing 0.1 M tetrabutylammonium hexafluorophosphate was used as solvent. The measurements were done under continuous flow of nitrogen. The concentration of the prepared samples was ca. 0.5 mM. Under these experimental conditions, the ferrocene oxidation was observed at 0.52 V.

Absorption measurements were carried out in a PerkinElmer Lambda 40 UV−vis spectrophotometer. Photoluminescence studies were done in a SPEX Fluorimeter. The emission spectra were corrected for the wavelength response of the detection system. Fluorescence lifetimes were performed with a LifeSpec-ps Fluorescence spectrometer from Edinburgh Instruments with a fixed excitation wavelength of 400 nm. For quantum yield measurements, the formula for optically dilute solutions was used.[30] Fluorescence quantum yields were determined by using perylene-3,4,9,10-tetracarboxylic tetrabutylester (ϕ_F = 0.98 in CH_2Cl_2) and *N,N′*-bis(1-hexylheptyl)-perylene bisimide (ϕ_F = 0.99 in CH_2Cl_2) as a reference.[31]

Pump−probe transient-absorption measurements were performed by using a tunable Yb:KGW laser system consisting of a YB:KGW laser (1028 nm) which operates at 5 kHz with a pulse duration of <180 fs (PHAROS-SP-06-200 Light Conversion) and an optical parametric amplifier (ORPHEUS-PO15F5HNP1, Light Conversion). A white light continuum probe pulse was generated by focusing part of the fundamental 1028 nm from Pharos into a sapphire crystal. Transient absorption data were collected using a commercial pump−probe spectrometer, HELIOS (Ultrafast Systems), in the wavelength range 490−910 nm. The maximum time-delay between the pump and the probe pulse was 3.3 ns. The compounds were dissolved in spectroscopic grade toluene, chloroform, and benzonitrile and placed in quartz cuvettes with a 2 mm path length. In order to prevent aggregation and photobleaching, the samples were stirred with a magnetic stirrer. The transient absorption spectra are taken in both parallel and perpendicular polarization angle between pump and probe light. Later, the data is averaged to a magic angle (~54.7°) to eliminate the polarization and photoselective effects.[32,33]

Transient absorption data was analyzed with global and target analysis using the open source software Glotaran.[34] TIMP is assuming that the time dependent spectra are a linear combination of difference absorption of various species with their respective population.[35] The Gaussian instrument response function, which is the account for dispersion and the coherent artifact, was taken into account while the analysis was carried out. The schemes in Figure 6 and Figure 8 were taken into account. The quality of fits and the relevance to correct species were compared with the global analysis of individual model compounds (see Figures S16−S21). Small deviations were observed due to different chemical surroundings, which can introduce slight shifts of transition energies or changes in oscillator strength.[36]

All calculations were performed by using Amsterdam Density Functional software.[37] The molecular structures in ground-state geometry were obtained by using the PBE functional with the DZP basis set. The molecules were charged +1, and geometry optimization was performed in the same functional and basis set as in the neutral molecule. The ionization potentials were obtained by subtracting the total bonding energies of neutral and cation.

RESULTS

Synthesis. The modular synthesis of the antenna molecules **D1A1**, **D1A2**, **D2A2**, **D2A3**, and **D3A3** and the synthesis of the model compounds **D1**−**D3** and **A1**−**A3** have been reported previously.[27] The synthesis and characterization of antenna molecule **D1A3** is given in the Supporting Information.

Electrochemical Studies. The redox potentials of the antenna systems and model compounds (V vs Fc/Fc^+) have been determined by cyclic voltammetry in anhydrous dichloromethane (ε_s = 8.93).[27] For the model acceptors **A1**, **A2**, and **A3**, reduction potentials E_{red} of −1.55, −1.33, and −1.08 V have been measured, indicating a more facile reduction as the acceptor gets more electron deficient. For the model donors **D2** and **D3**, oxidation potentials E_{ox} decrease from 0.80 to 0.75 V, indicating a more facile oxidation as the donor gets more electron-rich. The oxidation potential of the antenna containing **D1** is expected to be well above 0.80 V but could not be determined experimentally, as it is outside the measured potential window. We have determined the ionization energy of the donors, using DFT calculations and obtained values of 7.83, 7.42, and 7.37 eV for **D1**, **D2**, and **D3**, respectively. On the basis of the differences between these values, we estimate the oxidation potential of **D1** in DCM to be 1.2 eV and will use this value in the coming discussion.

The energies of photoinduced charge separation from the acceptor excited antenna systems ΔG^0_{CS} have been calculated using the Rehm−Weller expression based on the Born dielectric continuum model, eq 1:[38]

$$\Delta G^0_{CS} = [E_{ox}(D) - E_{red}(A)] - E_{00}(A) - \frac{e^2}{r_{DA}\varepsilon_s} + e^2\left(\frac{1}{2r_D} + \frac{1}{2r_A}\right)\left(\frac{1}{\varepsilon_s} - \frac{1}{\varepsilon_{ref}}\right) \quad (1)$$

In eq 1, $E_{ox}(D)$ and $E_{red}(A)$ are the oxidation potential of the donor and the reduction potential of the acceptor, measured in the reference solvent dichloromethane, while $E_{00}(A)$ is the spectroscopic excited-state energy of the acceptor. In this equation, r_D and r_A are the ionic radii of the donor and acceptor radical ions, r_{DA} is the donor−acceptor distance, while ε_{ref} and ε_s are the dielectric constants of the reference solvent dichloromethane and the chosen solvent, respectively. Using the Rehm−Weller equation is a crude approximation, as it assumes the formation of spherical ions and approaches the charge separation energy by point charges at the center to center distance between the chromophores r_{DA}. Because the

DOI: 10.1021/acs.jpcc.8b08503
J. Phys. Chem. C 2019, 123, 36−47

ionic radii r_D and r_A and the interchromophoric distance r_{DA} are of similar magnitude, it is difficult to determine what the effective charge separation distance is. The ionic radius of the perylene acceptor r_A = 7.4 Å was taken from the literature,[39] and for the ionic radius of the naphthalene acceptor r_D, a value of 3.5 Å was estimated. For the charge separation distance, r_{DA}, 10 Å was taken, a value intermediate between the center to center distance of 11.5 Å and the minimum interchromophoric distance of 6.5 Å. Margins of error were calculated using the uncertainties in r_A, r_D, and r_{DA}. In apolar toluene, the margins of error in the calculated charge separation energies are significant, due to the large contributions of the last terms in eq 1, whereas the values calculated for benzonitrile are more accurate.

Using eq 1, photoinduced charge separation energies ΔG^0_{CS} for all antenna molecules in dichlormethane were calculated. The obtained values indicate that for **D1A1**, **D1A2**, and **D1A3** there is no driving force for charge separation, whereas for **D2A2**, **D2A3**, and **D3A3** the driving force for charge separation is around −0.4 eV (Table 1). In toluene, the charge separation energies ΔG^0_{CS} are ∼0.45 eV higher than the corresponding values estimated for dichloromethane. This means that, within the large margin of error, charge separation from the perylene excited state is an energetically unfavorable process for all antenna molecules. Spectroscopic studies of these antenna compounds in toluene have already shown that none of the antenna molecules exhibited charge transfer from the excited acceptor state.[27] In chloroform, charge separation energies are approximately 0.3 eV lower than those in toluene. The values compiled in Table 1 indicate that the energy of charge separation is strongly negative, around −0.25 eV, for **D2A2**, **D2A3**, and **D3A3** only. In benzonitrile, charge separation energies are ∼0.25 eV lower than those in chloroform. Negative charge separation energies have been calculated for all antenna molecules, apart from **D1A1**, but strongly negative values, around −0.5 eV, have been calculated for **D2A2**, **D2A3**, and **D3A3** only.

Table 1. Energies of Charge Separation from the Excited Acceptor, Calculated Using eq 1

	ΔG^0_{CS} [a]			
comp	in Tol (eV) ± 0.18	in Chl (eV) ± 0.1	in DCM (eV) ± 0.05	in Bzn (eV) ± 0.03
D1A1	0.67	0.35	0.2	0.09
D1A2	0.49	0.17	0.03	−0.06
D1A3	0.46	0.14	−0.01	−0.11
D2A2	0.09	−0.23	−0.37	−0.46
D2A3	0.06	−0.27	−0.41	−0.51
D3A3	0.01	−0.30	−0.46	−0.56

[a]Driving force for charge separation with respect to the perylene singlet excited state, according to eq 1. Input data: r_D = 3.5 Å, r_A = 7.4 Å, r_{DA} = 10 Å, ε_{Tol} = 2.38, ε_{Chl} = 4.81, ε_{DCM} = 8.93, ε_{Bzn} = 25.9. Tol is toluene, Chl is chloroform, DCM is dichloromethane, and Bzn is benzonitrile.

On the basis of the calculated charge separation energies, electron transfer from the donor to the excited acceptor in polar solvents is expected to proceed in antenna molecules **D2A2**, **D2A3**, and **D3A3** only. The process becomes more exergonic, and is expected to go faster, in this order and upon increasing solvent polarity.

Energies of charge separation from the excited donor have been calculated as well and are compiled in Tables S1−S4. For compounds **D1A3**, **D2A2**, **D2A3**, and **D3A3**, charge separation energies are strongly negative, well below −0.4 eV in most cases. Therefore, charge transfer from the excited donor at appreciable rates is expected for these compounds. As this charge transfer process is in competition with ultrafast excitation energy transfer, it may not be observed unless both processes proceed at comparable rates.

Steady-State Absorption Studies. The absorption spectra of the reference compounds and antenna systems in benzonitrile are shown in Figure 2. Results obtained in chloroform are presented in Figure S4.

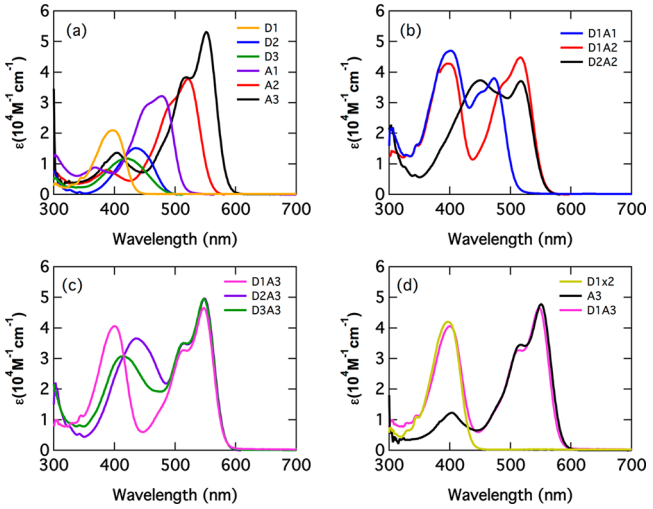

Figure 2. UV/vis absorption spectra in benzonitrile: (a) reference donor and acceptor compounds; (b) antenna systems **D1A1**, **D1A2**, and **D2A2**; (c) antenna systems **D1A3**, **D2A3**, and **D3A3**; (d) comparison of the absorption spectrum of antenna **D1A3** with those of the reference compounds **D1** and **A3**.

The donors **D1**−**D3** absorb in the visible region at 380−460 nm. Among them, **D1** has the most blue-shifted absorption. The absorption maxima are shifted to higher wavelengths by ca. 15−20 nm upon moving from **D1** to **D3** to **D2** (Table 2). In view of the stronger electron-donating nature of the dimethylamino group compared to the butylamino group, **D3** was expected to exhibit the most red-shifted absorption, not **D2**. The absorption spectra of the acceptors **A1**−**A3** are dominated by the characteristic strong $\pi-\pi^*$ transitions of the PTCA moieties in the region between 430 and 600 nm.[40,41] This absorption band shifts to longer wavelengths by ca. 40 nm, while the molar extinction coefficient increases strongly, upon moving from **A1** to **A2** to **A3** (Table 2).[41,42] Upon changing the solvent from benzonitrile to chloroform, only small blue shifts (5−10 nm) in the absorption maxima have been observed for both model acceptors and model donors (Table 2). This shows that the solvent polarity does not have a strong influence on the absorption properties of these molecules.

Most antenna systems exhibit good to excellent spectral coverage between 350 and 600 nm due to the complementary absorption of energy donor and acceptor chromophores (Figure 2b and c).[43] The contributions from donor and acceptor moieties can be easily seen in the absorption of antenna systems; i.e., the absorption at shorter wavelength is

DOI: 10.1021/acs.jpcc.8b08503
J. Phys. Chem. C 2019, 123, 36−47

Table 2. Optical Properties of Reference Compounds and Antenna Systems in Chloroform and Benzonitrile

compound	solvent	λ_{abs} (nm)	ε (M^{-1} cm^{-1})	λ_{em} (nm)	Φ_f[a]	τ_f[b] (ns)
D1	chloroform	396	20400	449	0.83	5.52
	benzonitrile	400	20600	461	0.66	5.40
D2	chloroform	427	15800	500	0.98	8.65
	benzonitrile	437	15200	514	0.87	8.29
D3	chloroform	411	11900	504	0.91	7.78
	benzonitrile	422	11700	516	0.40	4.90
A1	chloroform	477	35800	520	0.90	4.47
	benzonitrile	481	32100	523	0.85	4.25
A2	chloroform	516	40900	562	0.82	4.73
	benzonitrile	522	37800	573	0.79	4.73
A3	chloroform	546	55600	580	0.91	4.48
	benzonitrile	553	52900	590	0.86	4.47
D1A1	chloroform	405	48700	510	0.73[c]	4.27
		477	37900		0.76[d]	
	benzonitrile	402	47100	516	0.73[c]	4.23
		474	36300		0.75[d]	
D1A2	chloroform	395	46500	558	0.83[c]	4.42
		504	44400		0.85[d]	
	benzonitrile	400	42700	565	0.78[c]	4.35
		520	44200		0.77[d]	
D2A2	chloroform	441	38000	554	0.83[c]	4.62
		505	37800		0.80[d]	
	benzonitrile	448	37600	560	0.03[c]	0.49 (40%); 4.25 (60%)
		520	36900		0.05[d]	
D1A3	chloroform	397	42700	568	0.84[c]	3.71
		526	49400		0.83[d]	
	benzonitrile	398	42600	576	0.70[c]	3.05
		549	48500		0.68[d]	
D2A3	chloroform	427	39300	572	0.28[c]	1.36 (81%); 3.84 (19%)
		526	50500		0.26[d]	
	benzonitrile	437	36500	578	0.003[c]	0.17 (83%); 3.95 (17%)
		550	49400		0.005[d]	
D3A3	chloroform	418	32500	569	0.26[c]	0.98 (76%); 7.93 (24%)
		526	50100		0.26[d]	
	benzonitrile	418	30800	582	0.002[c]	0.21 (83%); 4.12 (17%)
		550	49000		0.001[d]	

[a]Fluoresence quantum yield, ±5% at $\Phi_F > 0.5$, ±10% at $0.5 > \Phi_F > 0.1$, ±20% at $\Phi_F < 0.1$. [b]Fluoresence lifetime (λ_{exc} = 400 nm). [c]Obtained after selective excitation of the naphthalene moiety. [d]Obtained after predominant excitation of the perylene moiety.

mainly from the naphthalene moieties, whereas the longer wavelength absorption is from the perylene part. The absorption spectra of all of the antenna systems are found to be almost equivalent to the sum of the absorption spectra of constituent chromophores (Figure 2d). This indicates the absence of ground state interaction between the energy donor and acceptor components, which is indeed expected because these chromophores are connected by nonconjugating rigid phenoxy linkers.

Steady-State and Time-Resolved Fluorescence Studies. Preliminary information regarding the excited-state interaction between naphthalene monoimide and perylene chromophores was obtained by the steady-state and time-resolved fluorescence spectroscopy. In general, both the naphthalene monoimide and the perylene model compounds are highly emissive with fluorescence quantum yields ranging from 0.80 to unity. Their fluorescence decay is monoexponential, and lifetimes are usually observed between 5−8 ns for NMI derivatives and 4−5 ns for PTCA-based compounds.[27,42]

The normalized fluorescence spectra of model donor and acceptor compounds in benzonitrile are given in Figure 3a, and the fluorescence quantum yields and lifetimes are summarized in Table 2. The model donor compound **D1** has the most blue-shifted emission with a maximum at 461 nm, whereas **D3** exhibits the most red-shifted emission spectrum (λ_{max} = 516 nm). The emission of **D2** is very similar to that of **D3** and is slightly blue-shifted by a few nanometers. A blue shift of 10−15 nm occurred for all of the model donors upon changing the solvent to chloroform (Figure S5a). All of the model donors are highly emissive in chloroform with fluorescence quantum yields higher than 0.80 and lifetimes between 5.52 and 8.65 ns. In benzonitrile, slightly reduced quantum yields and lifetimes have been observed for **D1** and **D2**. However, for **D3**, the fluorescence quantum yield and lifetime have significantly decreased to 0.40 and 4.90 ns, respectively.

The emission bands of reference acceptor compounds **A1**−**A3** are red-shifted compared to those of the reference donors (Figures 3a and S4a). Their fluorescence spectra exhibit a similar trend as in the case of absorption; i.e., red shifts are observed upon going from **A1** to **A2** to **A3**. All acceptor compounds are highly emissive with fluorescence quantum yields greater than 0.80 and lifetimes around 4.50 ns.

DOI: 10.1021/acs.jpcc.8b08503
J. Phys. Chem. C 2019, 123, 36−47

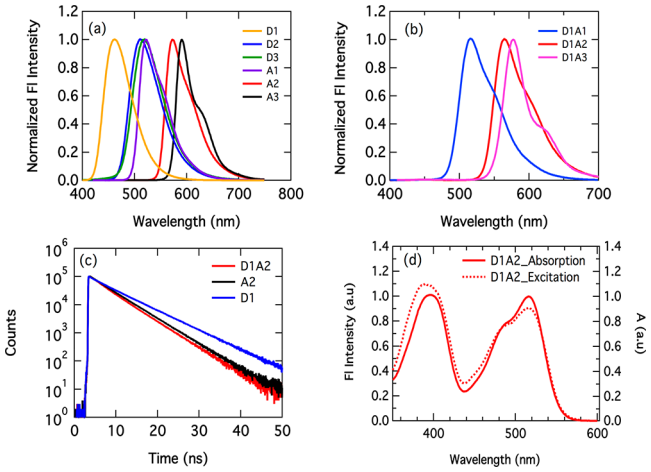

Figure 3. Normalized steady-state fluorescence spectra in benzonitrile of (a) model donor and acceptors and (b) antenna systems **D1A1**, **D1A2**, and **D1A3** after excitation of the naphthalene moiety. (c) Fluoresce decay time profiles of **D1A2** and its model compounds **D1** and **A2** in benzonitrile (λ_{ex} = 400 nm). (d) Excitation spectrum (dashed line) of **D1A2** measured at λ_{em} = 650 nm along with the absorption spectrum (solid line) in benzonitrile.

Fluorescence quantum yields are hardly affected by the solvent polarity for all of the model acceptors.

The antenna molecules were excited at two different wavelengths in order to perform emission studies after separate excitation of each chromophore. At first, antenna molecules were excited at the absorption maxima of the naphthalene chromophores at wavelengths around 410 nm. The characteristic emission of naphthalene moieties was found to be completely quenched for all of the antenna systems in both solvents (Figures 3b and S4b). This implies that the "slow" 5.0−8.5 ns fluorescence of the donor is completely outcompeted by other photoinduced processes. Energy transfer, which is known to be ultrafast in toluene, is the most obvious process, but electron transfer from the excited donor to the acceptor, which is an exergonic process according to our calculations, cannot be excluded *a priori*.

For the antennae **D1A1**, **D1A2**, and **D1A3** that contain the "electron poor" energy donor **D1**, the characteristic sensitized emission of perylene moieties was observed with fluorescence quantum yields and lifetimes identical to those observed when the antennae are excited at the acceptor chromophore (ca. 510 nm) (Figure 3b and c and Table 2). The fluorescence quantum yields and lifetimes of these antennae were also identical to those of the corresponding model acceptors **A1**−**A3**. These observations are explained by assuming quantitative exciton energy transfer (EET) from the donor part, followed by an undisturbed fluorescence of the acceptor part. This implies that other photoinduced processes, notably charge transfer processes, either from the excited donor or from the excited acceptor chromophore, do not take place at competing rates.[27] This is fully in line with the behavior of all antenna systems in toluene that we reported upon previously. The excitation spectra of **D1A1**, **D1A2**, and **D1A3**, measured at the perylene emission wavelength of ca. 600−650 nm, are identical to the absorption spectra of these compounds within the margin of error (Figures 3d, S5, and S6). This finding confirms that energy transfer from the donor to the acceptor is quantitative.

Entirely different results were obtained for the antenna systems **D2A3** and **D3A3**, which contain the amino functionalized "electron-rich" donors **D2** and **D3** along with the electron deficient PBI acceptor **A3**. Once more, the emission of the naphthalene part was completely quenched for these antenna systems, both in chloroform and in benzonitrile (Figures 4a and S4b). However, the fluorescence of the

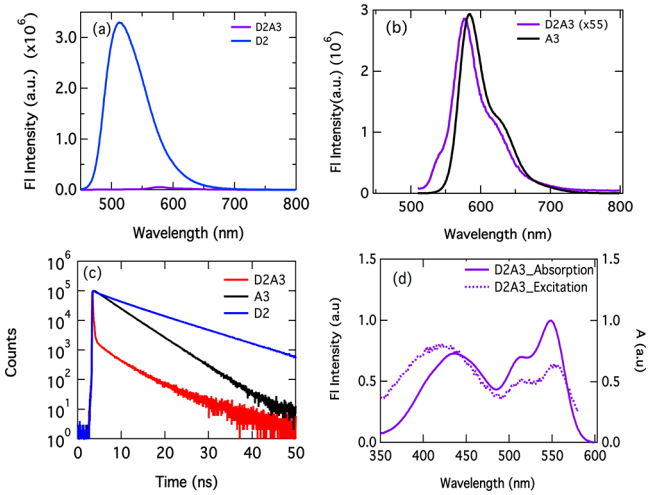

Figure 4. (a) Comparison between the steady-state emission of **D2A3** and **D2** in benzonitrile after predominant excitation of the donor part at 420 nm (A = 0.21 for both compounds). (b) Comparison between the steady-state emission of **D2A3** (multiplied 55 times) and **A3** in benzonitrile after selective excitation of the perylene part at 500 nm (A = 0.18 for both compounds). (c) Fluorescence decay curves of **D2A3** and its model molecules **D2** and **A3** in benzonitrile. (d) Excitation spectrum in benzonitrile (dashed line) of **D2A3** measured at λ_{em} = 650 nm along with the absorption spectrum (solid line) in benzonitrile.

perylene chromophore was also quenched for these compounds, not only when the donor was excited but also, and to the same extent, when the acceptor was excited (Figure 4b). The diminished emission from the excited acceptor chromophore implies that other quenching processes, most likely electron transfer from the donor toward the excited acceptor, take place at competitive rates. And finally, the identical quantum yields observed upon exciting either the donor or the acceptor chromophore in the antenna systems imply that energy transfer from the donor to the acceptor chromophore is quantitative. This conclusion is confirmed by excitation spectra of **D2A3** and **D3A3** that resemble the absorption spectra of these compounds (Figures 4d, S5, and S6).

For antenna molecules **D2A3** and **D3A3**, the quenching of perylene fluorescence was significantly increased upon moving from chloroform to benzonitrile. For example, in antenna **D2A3**, the fluorescence quantum yields Φ_F of the perylene chromophore were 0.26 and 0.005 in chloroform and benzonitrile, respectively (Table 2). Since increasing solvent polarity makes the charge-separated state thermodynamically more favorable, photoinduced charge transfer from the excited acceptor is the most likely quenching process.

The photophysical behavior of antenna system **D2A2** undergoes tremendous changes upon altering the solvent. In chloroform, the photophysics of **D2A2** was found to be very similar to that of **D1A1** and **D1A2**; i.e., upon excitation of the donor, efficient EET was observed, followed by an efficient acceptor emission. In contrast, in polar benzonitrile, fluorescence of the perylene acceptor was almost fully

DOI: 10.1021/acs.jpcc.8b08503
J. Phys. Chem. C 2019, 123, 36−47

quenched, which is indicative of an efficient nonradiative deactivation of the excited acceptor chromophore, as was seen in the case of antenna systems **D2A3** and **D3A3**. This polarity effect once more points toward the involvement of charge transfer from the excited acceptor. For this process, the driving force, going from chloroform to benzonitrile, doubles from −0.23 to −0.43 eV, according to our calculations (Table 1).

From the steady-state and time-resolved fluorescence experiments (Figures 3d, 4c, and S7), rates of fluorescence quenching can be determined, using eq S1.[44] For **D2A3** and **D3A3** in chloroform, rates of fluorescence quenching of (5−6) × 10^8 s^{-1} have been calculated, which is in the same order as the rates of fluorescence. For **D2A2** and **D2A3** in benzonitrile, quenching rates k_Q of 8 × 10^9 and 4 × 10^{10} s^{-1} have been calculated. These quenching rates were calculated on the basis of very low and thus highly inaccurate fluorescence quantum yields but correlate well with the rates obtained by transient absorption spectroscopy, *vide infra*.

Femtosecond Transient Absorption Studies. Femtosecond transient absorption spectroscopy (TAS) studies were carried out to gain further insight into the excited-state dynamics of the antenna molecules. For these studies, all antennae along with model compounds were investigated in chloroform and benzonitrile. Measurements were conducted at two different excitation wavelengths to excite the donor and acceptor components separately. The excitation wavelengths corresponding to the absorption maxima of the PTCA acceptor were used for selective excitation of the perylene component. Selective excitation of the NMI donor chromophore, however, was not possible because PTCAs also absorb at ca. 410 nm, i.e., the absorption maximum of the naphthalene donor. Therefore, the predominant excitation of the donor part was achieved by selecting the excitation wavelengths with the highest ratio of donor versus acceptor absorption. The extent of acceptor absorption at short wavelengths was taken into account with the data analysis.

TAS measurements were carried out on the reference acceptor compounds (**A1**−**A3**). As an example, the excitation of **A3** in benzonitrile is shown in Figure 5a. Excitation of **A3** resulted in an immediate formation of the first singlet excited state of the perylene chromophore that is characterized by its typical strong absorption between 650 and 900 nm and a bleach of the ground state absorption around 550 nm.[9,25,27,45] Furthermore, a negative band corresponding to the stimulated emission of the perylene chromophore was seen around 600 nm. With the increase in delay times, the characteristic absorption of the perylene singlet excited state remained at the same wavelength (ca. 700 nm) and slowly decayed with a time constant corresponding to the fluorescence of the perylene chromophore (∼4.5 ns). Small spectral changes were observed in the bleach region between 525 and 650 nm, including a significant loss of amplitude, which were most pronounced at ca. 100 ps delay. These spectral changes are attributed to vibrational relaxation of the excited perylene chromophore, possibly in combination with solvent relaxation processes.[46,47] Similar results were obtained for all of the reference acceptor compounds in both chloroform and benzonitrile (Figure S10).

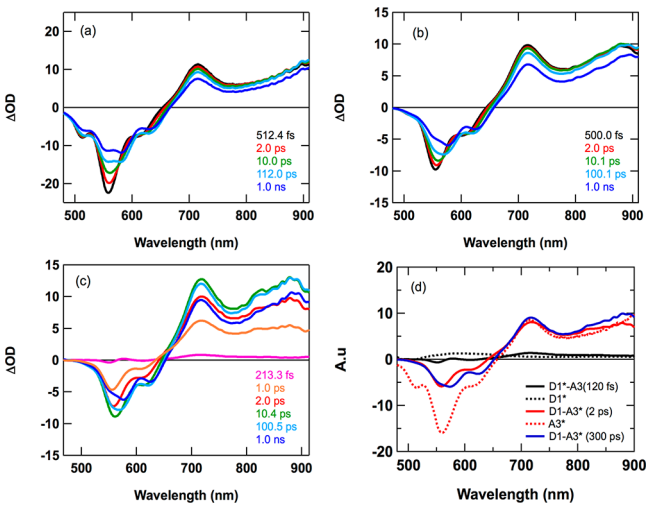

Figure 5. Transient absorption spectra in benzonitrile: (a) **A3** and (b) **D1A3** after selective excitation of perylene chromophore at 540 nm; (c) **D1A3** after predominant excitation of the naphthalene part at 400 nm; (d) **D1A3** spectra (excited at 400 nm) along with those of **D1** and **A3**.

Subsequently, TAS measurements were carried out on the antenna systems **D1A1**, **D1A2**, and **D1A3**. The antennae were first selectively excited at their perylene absorption maxima, which resulted in transient absorption spectra similar to those of the respective reference acceptor compounds, as is illustrated for antenna **D1A3** in Figure 5b. In the bleach region, small changes were observed in the picosecond time scale due to relaxation of the excited perylene. The positive absorption bands between 700 and 900 nm remained unchanged at picosecond delay times and, eventually, started to decrease at nanosecond delay times. This leads to the conclusion that, for these antenna systems, the perylene excited state decays to the ground state in the same manner as in the model acceptor, *via* emission from the singlet excited state. Thus, for these compounds, even in the polar solvent benzonitrile, charge transfer processes have not been detected (Figures S10 and S11).

Upon excitation of these antenna molecules at ca. 400 nm, as illustrated for antenna **D1A3**, immediate formation of the donor's excited state, along with the excited acceptor, was observed at femtosecond delay times (Figure 5c and d). Subsequently, the perylene excited-state absorption increased with further increase in delay times in the range 0−10 ps. At nanosecond delay times, the magnitude of the perylene absorption gradually decreased. The swift increase in absorption at picosecond delay times is consistent with fast EET from the naphthalene donor to the perylene acceptor and the decrease at nanosecond delay times with the subsequent slow decay of perylene excited state to the ground state via fluorescence. No signs of charge separation, i.e., the characteristic sharp absorption of the perylene radical anion at ca. 700 nm,[46,25] were observed (Figures S10 and S11, Supporting Information). The photophysical pathways taking place in these antenna systems (**D1A1**, **D1A2**, and **D1A3**) after donor excitation are summarized in Figure 6.

Similar measurements were carried out for the antenna systems **D2A2**, **D2A3**, and **D3A3**, which contain relatively electron-rich energy donors (**D2** and **D3**) and the moderately and highly electron deficient acceptors **A2** and **A3**. At first, measurements were performed in polar benzonitrile in which the perylene emission of the antenna systems was almost entirely quenched. In Figure 7a, the time-resolved absorption of **D2A3** after selective irradiation of the perylene chromophore at 540 nm is shown. Immediate formation of the perylene excited state, characterized by the positive

DOI: 10.1021/acs.jpcc.8b08503
J. Phys. Chem. C 2019, 123, 36−47

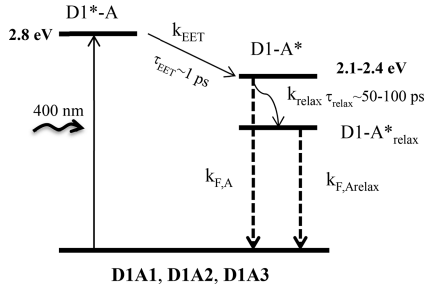

Figure 6. Kinetic scheme describing the photophysical processes occurring upon excitation of **D1** in antenna systems **D1A1**, **D1A2**, and **D1A3** in chloroform and benzonitrile. Representative time constants are given for the photophysical processes.

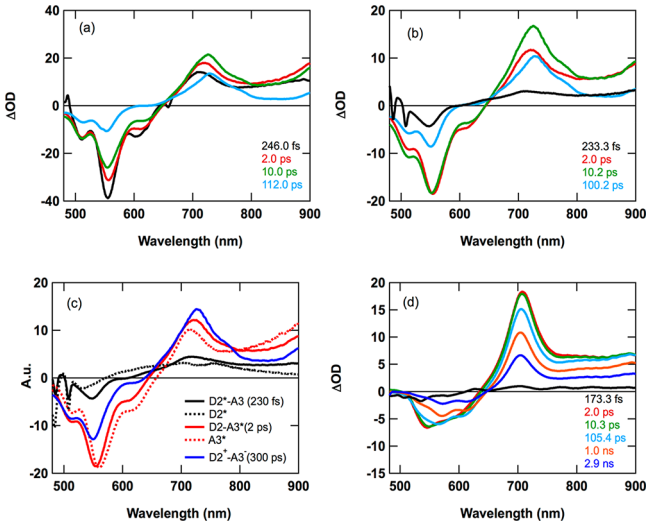

Figure 7. Transient absorption spectra of antenna **D2A3** in benzonitrile (a) after selective excitation of **A3** at 540 nm and (b) after excitation of **D2** at 440 nm; (c) comparison between the spectra of **D2** and **A3**; (d) **D2A3** after excitation at 440 nm in chloroform.

absorption between 700 and 900 nm with a maximum at 705 nm, was observed. This absorption remained practically the same (apart from a red shift of maxima) with a further increase in evolution time in the range 1−10 ps. At longer delay times (ca. 100 ps), two noticeable changes appeared in the transient absorption spectra. The positive absorption between 700 and 900 nm significantly sharpened, developing a maximum at 730 nm, which is a characteristic signature of the perylene bisimide radical anion.[48,25] Second, the stimulated emission at 610 nm completely vanished, which is indicative of the formation of a nonemissive excited state. These spectral changes have been attributed to the formation of a charge separated state. This conclusion is in line with the strong fluorescence quenching that was observed for **D2A3** in benzonitrile. Similar spectra were recorded for compounds **D2A2** and **D3A3** in Figures S12 and S13.

When the naphthalene chromophore of antennae **D2A2**, **D2A3**, and **D3A3** was excited using 440 nm laser light, the spectroscopic signature of the singlet excited state of the donor, along with that of the acceptor, appeared in the femtosecond time scale, as is illustrated for compound **D2A3** in Figure 7b. Subsequently, the perylene singlet excited-state absorption increased at delay times in the range 0−10 ps. At ca. 100 ps delay, the spectrum significantly changed, with the sharpening of the positive absorption at ~730 nm and the disappearance of the stimulated emission band at ca. 610 nm. These features are exactly the same as those obtained after the selective excitation of the PBI at 540 nm (Figure 7a). To summarize, upon donor excitation of antennae **D2A2**, **D2A3**, and **D3A3**, D*A is formed instantaneously. Subsequently, the donor transfers its energy to the acceptor within a few picoseconds, forming DA*. Eventually, charge transfer occurs to form the charge-separated state, $D^{\bullet+}A^{\bullet-}$, which recombines to the ground state at the nanosecond time scale. It is important to mention that we did not observe any signature of the relaxation of the excited perylene in the transient absorption spectra of **D2A3** and **D3A3** in benzonitrile. However, in the case of **D2A2**, where the charge transfer process is considerably slower, the relaxation of the locally excited perylene precedes charge transfer. The photophysical pathways taking place in **D2A2**, **D2A3**, and **D3A3**, in benzonitrile, after donor excitation are summarized in Figure 8.

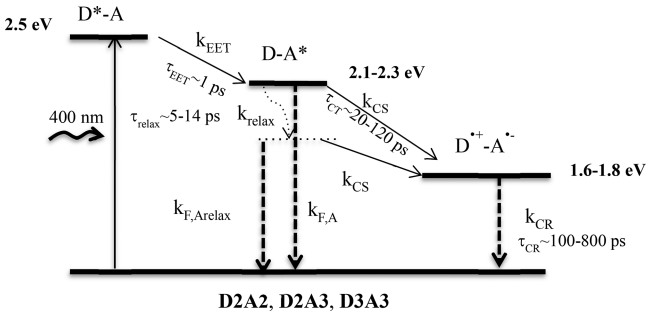

Figure 8. Kinetic scheme describing the photophysical processes upon excitation of donor (at 440 nm) for compounds **D2A2**, **D2A3**, and **D3A3** in benzonitrile. Representative time constants are given for the photophysical processes.

In less polar chloroform, as illustrated for compound **D2A3** in Figure 7d, no spectral evidence for the formation of a charge transfer state was detected, i.e., by the characteristic absorption of perylene radical anion and loss of stimulated emission. The perylene excited state was clearly seen, even after 2 ns delay times in the transient absorption spectra. This suggests that the perylene singlet excited state decays to the ground state by fluorescence. However, from the steady-state measurements, it is known that the fluorescence of the acceptor fluorescence in **D2A3** (Φ_F ~ 0.25) is severely quenched compared to that of **A3** (Φ_F~ 0.9). The fact that the charge-separated state is not visible in this case may be due to a fast charge recombination, which prevents buildup of this species. In addition, the fact that the rate of fluorescence and the rate of charge transfer are comparable impedes detection of a charge-separated state. Contrary to the measurements in benzonitrile, we were also able to notice the relaxation process of the perylene chromophore for all of the antenna systems in chloroform. This is attributed to the fact that charge separation in chloroform is slower than that in benzonitrile and therefore cannot outcompete the relaxation of the excited perylene singlet excited state.

Rates of Energy and Charge Transfer. We have previously analyzed the photophysics of the antenna systems in toluene by a single wavelength analysis.[27] In this specific case, single wavelength data analysis was allowed because the photophysics of these antenna molecules in toluene is very straightforward, without the involvement of competing charge transfer processes. However, because in polar solvents multiple

DOI: 10.1021/acs.jpcc.8b08503
J. Phys. Chem. C 2019, 123, 36−47

photophysical processes occur after donor excitation, and several species are formed, the rates of these processes could not be derived from changes in absorption at a single wavelength. Therefore, global and target analysis was performed by taking into account the rates of individual processes obtained from the model compounds along with the optical densities of donor and acceptor moieties at the excitation wavelengths. The open software package Glotaran[36] was used, and further details are provided in the Supporting Information. Analysis of the TAS data by global and target analysis was performed only for the benzonitrile case, because the analysis of the TAS data obtained in chloroform was severely hampered by the presence of CH Raman peaks in the absorption spectra. In order to find the rates of excited energy transfer k_{EET}, acceptor relaxation k_{relax}, charge separation k_{CS}, and charge recombination k_{CR}, the rates of the fluorescence decay of the donor ($k_{F,D}$) and the rates of the fluorescence decay of the acceptor ($k_{F,A}$, $k_{F,Arelax}$) are taken from the global analysis of model compounds and kept constant in the target analysis of the antenna, similar to the approach reported by Gorczak et al.[36]

The kinetic scheme of photophysical processes for **D1A1**, **D1A2**, and **D1A3** in benzonitrile is given in Figure 6, and that for **D2A2**, **D2A3**, and **D3A3** in the same solvent is given in Figure 8. The initially excited donor (D*) undergoes energy transfer within a couple of picoseconds with a rate characterized by the time constant τ_{EET}. For all antenna molecules, this process is the first photophysical process that occurs. From the steady-state fluorescence measurements, that all show fluorescence quantum yields independent of the excitation wavelength, it is clear that charge transfer from the excited donor is insignificant, i.e., outcompeted by the ultrafast energy transfer.

For compounds **D1A1**, **D1A2**, and **D1A3**, the excited acceptor part undergoes a relaxation process. This relaxation has also been seen in the model acceptors, albeit with different rate constants. Both the A* and A*$_{relax}$ singlet excited states decay to the ground state via fluorescence.

The time constants and rate constants of the photophysical processes in benzonitrile, as determined by global analysis, are compiled in Tables 3 and S5. From Table 3, it can be concluded that excited energy transfer is ultrafast for all antenna systems, with time constants τ_{EET} between 740 fs and 1.39 ps. The modest differences in τ_{EET} values may be explained by differences in the overlap integrals and acceptor extinction coefficients, *vide infra*. The charge separation rates reported in Table 3 are in line with the Rehm−Weller behavior; i.e., they increase as the charge separation energy ΔG^0_{CS} increases. Also, charge transfer is not observed if the calculated charge separation energies ΔG^0_{CS}, depicted in Table 1, are above −0.2 eV. For compounds **D2A2**, **D2A3**, and **D3A3**, charge recombination rates are lower than the charge separation rates, by a factor of 2−25, which results in buildup and subsequent detection of the charge separated states. For these charge recombination rates, no obvious correlation with molecular structure has been observed. For the relaxation rates of the acceptor singlet excited state, k_{relax} no, obvious correlation with the molecular structure is apparent either.

Table 3. Time Constants of All Photophysical Processes Determined from Transient Absorption after Donor Excitation in Benzonitrile

comp	τ_{relax} (ps)	τ_{EET} (ps)	τ_{CS} (ps)	τ_{CR} (ps)
D1A1	57.9	1.16		
D1A2	52.1	1.39		
D1A3	97.8	1.10		
D2A2	14.3	0.91	117.5	345
D2A3	5.58	0.74	32.3	800
D3A3		0.79	17.4	106

In Tables 3 and S6, the kinetic data regarding the energy and charge transfer rates of the six antenna molecules in toluene, chloroform, and benzonitrile are compiled. For the energy transfer rates, the values in the different solvents as well as the trends within each solvent are strikingly similar. The influence of molecular structure on energy transfer rates is modest as well.

The influence of molecular structure on charge separation rates is strong and determined by the excitation energy of the acceptor chromophore and the redox properties of the donor and acceptor chromophores in a straightforward manner. The effect of the solvent is also very pronounced, as an increase in solvent polarity specifically stabilizes the charge-separated state, according to eq 1. To show this we have performed TAS measurements in solvents of varying polarity, as summarized in Table 4. In apolar toluene, no charge separation is observed, while, in chloroform, charge separation is seen in two cases only, with rates comparable to those of acceptor fluorescence. Only in polar benzonitrile fast charge separation that is able to outcompete fluorescence has been observed.

Table 4. Time Constants of Energy and Charge Transfer Processes in Toluene, Chloroform, and Benzonitrile

comp	$\tau_{EET(Tol)}$ (ps)	$\tau_{EET(Chl)}$ (ps)	$\tau_{EET(Bzn)}$ (ps)	$\tau_{CS(Chl)}$ (ps)	$\tau_{CS(Bzn)}$ (ps)
D1A1	0.99	1.02	1.12		
D1A2	1.31	1.38	1.39		
D1A3	1.07	1.10	1.16		
D2A2	1.16	1.10	0.90		118
D2A3	0.92	0.66	0.74	2000	32
D3A3	0.87	0.90	0.79	1700	17

DISCUSSION

The results obtained by the photophysical measurements in the solvents toluene, chloroform, and benzonitrile provide a clear picture of the photochemical processes that take place upon excitation of the investigated antenna molecules.

In toluene, all antenna molecules exhibited a fast energy transfer ($\tau_{EET} \sim 1$ ps) after donor excitation, followed by intense acceptor fluorescence ($\tau_F \sim 5$ ns). In this solvent, photoinduced charge transfer is absent for all compounds. In chloroform, the increased solvent polarity did not change the photophysical behavior of the antenna molecules containing the acceptor units **A1** and **A2**. Fast energy transfer and highly efficient fluorescence were observed after donor excitation. Only for compounds with the strongly electron deficient PBI acceptor **A3**, significant fluorescence quenching was observed due to a relatively slow photoinduced charge transfer process ($\tau_{CS} \sim 1.7$−2 ns). Charge separated states were not observed in chloroform by TAS measurements, and this may be due to fast charge recombination. In benzonitrile, the antenna molecules containing the weakest electron donating energy donor **D1** did not undergo photoinduced charge transfer at all.

DOI: 10.1021/acs.jpcc.8b08503
J. Phys. Chem. C 2019, 123, 36−47

For the remaining antenna molecules **D2A2**, **D2A3**, and **D3A3**, fluorescence quenching was almost quantitative, due to a fast photoinduced charge separation from the excited acceptor.

The photophysical behavior of our antenna can be accurately tuned by changing the molecular structure and solvent polarity, and these changes are predictable and fairly well understood. Excitation energy transfer is always fast, in the 1 ps range, is modestly influenced by the molecular structure, and is unaffected by the solvent. The fastest energy transfer is observed for **D2A3** and **D3A3**, followed by **D2A2**, **D1A1**, and **D1A3**. In all cases, **D1A2** is slower, but the difference between the EET rates is modest, ±30%. The differences in EET rates between the antenna molecules can be explained if we assume that the excited energy transfer proceeds through the Förster mechanism (eq S2) and that the conformation of the rigid antenna molecules is not solvent dependent. Inspection of eq S2 reveals that differences in overlap integrals J, more specifically the overlap of normalized donor emission and acceptor absorption spectra, and differences in absorption cross section, quantified by extinction coefficients ε_A, explain the observed trend in excited energy transfer rates. For example, faster energy transfer for **D2A2** than for **D1A2** is explained by a better overlap of normalized donor emission and acceptor absorption, while the trend in acceptor extinction coefficients, **A3** > **A2** > **A1**, explains the general trend in energy transfer rates for antenna molecules with identical donors.

Photoinduced charge transfer from the excited acceptor takes place when the calculated values of the charge separation energy ΔG^0_{CS} are strongly negative. Rates of this process correlate with calculated charge separation energies ΔG^0_{CS} (Table 1). For example, in benzonitrile, the order of charge separation rates k_{CS}, **D3A3** > **D2A3** > **D2A2**, is in accordance with the trend in calculated charge separation energies ΔG^0_{CS}. Also, calculated ΔG^0_{CS} values of these compounds in chloroform are significantly lower than those in benzonitrile, and the same is true for the k_{CS} values. From the data in Table 1, it is also clear that the CS processes are only observed when ΔG^0_{CS} values are below −0.2 eV, which is an apparent threshold for this process. Tuning the charge separation energy ΔG^0_{CS} is achieved by structural modification of the antennae, i.e., using different donor−acceptor combinations, and by changing the solvent polarity, which influences the stability of the charge separated state relative to those of the other states (eq 1). Finally, It should be noted that **D1A1**, **D1A2**, and **D1A3**, to the best of our knowledge, are the only PTCA-based antenna molecules in which intramolecular photoinduced electron transfer is absent in all tested solvents, including polar benzonitrile. This demonstrates that incorporating the electron poor energy donor **D1** in the antenna molecule fully suppresses intramolecular charge transfer. However, the substitution of the strongly electron deficient PBI acceptor **A3** by its less electron deficient counterparts PMIDE **A2** or the PTE **A1** is also an important modification for diminishing photoinduced charge transfer.

Charge separated states have been detected in benzonitrile only, and charge recombination rates have been determined for the antenna molecules **D2A2**, **D2A3**, and **D3A3**. For the charge recombination rates k_{CR}, the order **D2A3** > **D2A2** > **D3A3** has been observed (Tables 3 and S4). In all cases, charge separation was faster than charge recombination. For **D2A3**, $k_{CS}/k_{CR} \sim 25$, and for this compound, the charge separated state is best visible in the transient absorption spectra.

On the basis of strong, tunable absorption in the visible region, ultrafast excited energy transfer, and tunable charge transfer within the antenna systems, the light harvesting antenna molecules presented here are very well suited for the construction of devices for artificial photosynthesis.[2] For incorporation into larger antenna systems, that contain an additional red-shifted acceptor, all antenna molecules appear to be well-suited. This is based on the assumption that energy transfer to an additional acceptor will be ultrafast and should outcompete charge transfer within the antenna molecules. Compounds **D1A1**, **D2A1**, and **D1A3** are particularly suited for this purpose, as these assemblies do not exhibit charge transfer within the antenna assembly under all investigated conditions.

In devices for artificial photosynthesis,[49] charge transfer should take place from an energy acceptor chromophore, referred to as the sensitizer, toward charge separator units. Efficient device operation will take place only if these desired charge transfer processes, which drive the catalytic reactions, outcompete other processes that may occur from the excited acceptor. In the antenna molecules investigated here, energy transfer takes place from donors attached at bay positions, while peri positions are available for attaching charge-separating units. Previous research on the photophysics of PTCA derivatives, however, has shown that rates of photoinduced charge transfer processes from bay positions[42,44,50] are 1 order of magnitude faster than those from imides at the peri positions. This implies that charge separators should preferably be attached at bay positions, which facilitate a faster charge transfer. Therefore, additional bay substituents for attaching charge separators should be attached to the antenna systems presented here. This can be achieved by starting the antenna synthesis from tetrachloro-[41,51] instead of dibromoperylenes and by implementing the recently developed chemistry for regioselective substitution of bay halogens.[52]

CONCLUSIONS

Six artificial light-harvesting antenna systems with tunable optical and electrochemical properties, composed of naphalene monoimide energy donors attached to the bay positions of perylene 3,4,9,10-tetracarboxylic acid derived acceptor parts, were investigated by cyclic voltammetry and steady-state and time-resolved spectroscopy in solvents of different polarity. All of the antenna molecules exhibit a strong absorption in a large part of the visible region by complementary absorption of the donor and acceptor constituents. Excited energy transfer from the donor to the acceptor was quantitative and ultrafast for all antenna molecules in all solvents, with time constants τ_{EET} ranging from 0.7 to 1.4 ps. This process was hardly depending on solvent polarity and was only modestly influenced by molecular structure.

Charge transfer, from the excited acceptor, was strongly dependent on both the molecular structure and the solvent polarity. In toluene, this process is absent for all antenna molecules, and after ultrafast excitation energy transfer from the donor to the acceptor, only emission from the acceptor is observed. In chloroform only for **D2A3** and **D3A3**, the molecules with the stronger electron donors **D2** and **D3** and the strongest electron acceptor **A3**, charge transfer, from the excited acceptor, was observed. Charge separation rates were relatively low, $\tau_{CS} \sim 1.7-2$ ns, and comparable with the rate of

DOI: 10.1021/acs.jpcc.8b08503
J. Phys. Chem. C 2019, 123, 36−47

acceptor fluorescence. In benzonitrile, fast charge separation was observed for antenna **D2A2**, **D2A3**, and **D3A3**, $\tau_{CS} \sim 20-120$ ps. CS rates correlated well with the calculated free energy of charge separation ΔG^0_{CS}. The acceptor radical anion was detected for these compounds by TAS, and charge recombination rates, $\tau_{CR} \sim 100-800$ ps, were determined.

For antenna molecules **D1A1**, **D1A2**, and **D1A3**, *ideal antenna behavior* was observed, i.e., fast excited energy transfer and no charge transfer or other competing processes, not even in polar benzonitrile. This makes these molecules extremely suitable for incorporation in devices for artificial photosynthesis.

Our current research is focused on incorporating antenna molecules in larger antenna assemblies and on changing the antenna design by attaching energy donors to imides at peri positions, while keeping the bay positions available for charge transfer.

■ ASSOCIATED CONTENT

Supporting Information

The Supporting Information is available free of charge on the ACS Publications website at DOI: 10.1021/acs.jpcc.8b08503.

Synthesis and characterization of **D1A3**; molecular structures of the model compounds; energies of charge separation; steady-state absorption and emission spectra of all compounds in chloroform; excitation spectra and fluorescence decay curves in chloroform and benzonitrile; transient absorption spectra of model compounds and antenna molecules in chloroform; rate constants of photophysical processes; details of global and targeted analysis (PDF)

■ AUTHOR INFORMATION

Corresponding Authors

*E-mail: W.F.Jager@tudelft.nl.
*E-mail: F.C.Grozema@tudelft.nl.

ORCID

Rajeev K. Dubey: 0000-0001-5165-7801
Wolter F. Jager: 0000-0001-7664-6949
Ferdinand C. Grozema: 0000-0002-4375-799X

Notes

The authors declare no competing financial interest.

■ ACKNOWLEDGMENTS

Financial support from the Foundation for Fundamental Research on Matter, which is part of The Netherlands Organization for Scientific Research, is gratefully acknowledged. This research has also received funding from the European Research Council Horizon 2020 ERC Grant No. 648433.

■ REFERENCES

(1) Harriman, A. Artificial Light-harvesting Arrays for Solar Energy Conversion. *Chem. Commun.* **2015**, *51*, 11745−11756.
(2) Frischmann, P. D.; Mahata, K.; Wurthner, F. Powering the Future of Molecular Artificial Photosynthesis with Light-harvesting Metallosupramolecular Dye Assemblies. *Chem. Soc. Rev.* **2013**, *42*, 1847−1870.
(3) Swierk, J. R.; Mallouk, T. E. Design and Development of Photoanodes for Water-splitting Dye-sensitized Photoelectrochemical Cells. *Chem. Soc. Rev.* **2013**, *42*, 2357−2387.
(4) Jradi, F. M.; O'Neil, D.; Kang, X.; Wong, J.; Szymanski, P.; Parker, T. C.; Anderson, H. L.; El-Sayed, M. A.; Marder, S. R. A Step Toward Efficient Panchromatic Multi-Chromophoric Sensitizers for Dye Sensitized Solar Cells. *Chem. Mater.* **2015**, *27*, 6305−6313.
(5) Meyer, T. J. Chemical Approaches to Artificial Photosynthesis. *Acc. Chem. Res.* **1989**, *22*, 163−170.
(6) Wasielewski, M. R. Photoinduced Electron Transfer in Supramolecular Systems for Artificial Photosynthesis. *Chem. Rev.* **1992**, *92*, 435−461.
(7) Scholes, G. D.; Fleming, G. R.; Olaya-Castro, A.; van Grondelle, R. Lessons From Nature About Solar Light Harvesting. *Nat. Chem.* **2011**, *3*, 763−774.
(8) Iehl, J.; Nierengarten, J.-F.; Harriman, A.; Bura, T.; Ziessel, R. Artificial Light-Harvesting Arrays: Electronic Energy Migration and Trapping on a Sphere and between Spheres. *J. Am. Chem. Soc.* **2012**, *134*, 988−998.
(9) Flamigni, L.; Ventura, B.; You, C.-C.; Hippius, C.; Würthner, F. Photophysical Characterization of a Light-Harvesting Tetra Naphthalene Imide/Perylene Bisimide Array. *J. Phys. Chem. C* **2007**, *111*, 622−630.
(10) Fron, E.; Puhl, L.; Oesterling, I.; Li, C.; Müllen, K.; De Schryver, F. C.; Hofkens, J.; Vosch, T. Energy Transfer Pathways in a Rylene-Based Triad. *ChemPhysChem* **2011**, *12*, 595−608.
(11) Ziessel, R.; Ulrich, G.; Haefele, A.; Harriman, A. An Artificial Light-Harvesting Array Constructed from Multiple Bodipy Dyes. *J. Am. Chem. Soc.* **2013**, *135*, 11330−11344.
(12) Zhang, J.; Fischer, M. K. R.; Bäuerle, P.; Goodson, T. Energy Migration in Dendritic Oligothiophene-Perylene Bisimides. *J. Phys. Chem. B* **2013**, *117*, 4204−4215.
(13) Fujitsuka, M.; Harada, K.; Sugimoto, A.; Majima, T. Excitation Energy Dependence of Photoinduced Processes in Pentathiophene−Perylene Bisimide Dyads with a Flexible Linker. *J. Phys. Chem. A* **2008**, *112*, 10193−10199.
(14) Dinçalp, H.; Kızılok, Ş.; İçli, S. Fluorescent Macromolecular Perylene Diimides Containing Pyrene or Indole Units in Bay Positions. *Dyes Pigm.* **2010**, *86*, 32−41.
(15) Davis, K. M. C. Solvent Effects on Charge-transfer Fluorescence Bands. *Nature* **1969**, *223*, 728−728.
(16) Wurthner, F. Perylene Bisimide Dyes as Versatile Building Blocks for Functional Supramolecular Architectures. *Chem. Commun.* **2004**, *14*, 1564−1579.
(17) Huang, C.; Barlow, S.; Marder, S. R. Perylene-3,4,9,10-tetracarboxylic Acid Diimides: Synthesis, Physical Properties, and Use in Organic Electronics. *J. Org. Chem.* **2011**, *76*, 2386−2407.
(18) Langhals, H.; Saulich, S. Bichromophoric Perylene Derivatives: Energy Transfer from Non-Fluorescent Chromophores. *Chem. - Eur. J.* **2002**, *8*, 5630−5643.
(19) Hippius, C.; Schlosser, F.; Vysotsky, M. O.; Böhmer, V.; Würthner, F. Energy Transfer in Calixarene-Based Cofacial-Positioned Perylene Bisimide Arrays. *J. Am. Chem. Soc.* **2006**, *128*, 3870−3871.
(20) Gómez, R.; Segura, J. L.; Martín, N. Highly Efficient Light-Harvesting Organofullerenes. *Org. Lett.* **2005**, *7*, 717−720.
(21) Hurenkamp, J. H.; Browne, W. R.; Augulis, R.; Pugzlys, A.; van Loosdrecht, P. H. M.; van Esch, J. H.; Feringa, B. L. Intramolecular Energy Transfer in a Tetra-coumarinperylene System: Influence of Solvent and Bridging Unit on Electronic Properties. *Org. Biomol. Chem.* **2007**, *5*, 3354−3362.
(22) Ryan, S. T. J.; Del Barrio, J.; Ghosh, I.; Biedermann, F.; Lazar, A. I.; Lan, Y.; Coulston, R. J.; Nau, W. M.; Scherman, O. A. Efficient Host−Guest Energy Transfer in Polycationic Cyclophane−Perylene Diimide Complexes in Water. *J. Am. Chem. Soc.* **2014**, *136*, 9053−9060.
(23) van Stokkum, I. H. M.; Lozier, R. H. Target Analysis of the Bacteriorhodopsin Photocycle Using a Spectrotemporal Model. *J. Phys. Chem. B* **2002**, *106*, 3477−3485.
(24) Sautter, A.; Kaletaş, B. K.; Schmid, D. G.; Dobrawa, R.; Zimine, M.; Jung, G.; van Stokkum, I. H. M.; De Cola, L.; Williams, R. M.; Würthner, F. Ultrafast Energy-Electron Transfer Cascade in a

DOI: 10.1021/acs.jpcc.8b08503
J. Phys. Chem. C 2019, 123, 36−47

Multichromophoric Light-Harvesting Molecular Square. *J. Am. Chem. Soc.* **2005**, *127*, 6719−6729.
(25) Dubey, R. K.; Niemi, M.; Kaunisto, K.; Stranius, K.; Efimov, A.; Tkachenko, N. V.; Lemmetyinen, H. Excited-State Interaction of Red and Green Perylene Diimides with Luminescent Ru(II) Polypyridine Complex. *Inorg. Chem.* **2013**, *52*, 9761−9773.
(26) Dyar, S. M.; Smeigh, A. L.; Karlen, S. D.; Young, R. M.; Wasielewski, M. R. Photo-initiated Multi-step Electron Transfer in Donor−Acceptor Systems Using a Novel bi-functionalized Perylene Chromophore. *Chem. Phys. Lett.* **2015**, *629*, 23−28.
(27) Dubey, R. K.; Inan, D.; Sengupta, S.; Sudholter, E. J. R.; Grozema, F. C.; Jager, W. F. Tunable and Highly Afficient Light-harvesting Antenna Systems Based on 1,7-perylene-3,4,9,10-Tetracarboxylic Acid Derivatives. *Chem. Sci.* **2016**, *7*, 3517−3532.
(28) For PTEs, high thermal and photochemical stability have been reported. See: (a) Jiang, Y.; Lu, L.; Yang, M.; Zhan, C.; Xie, Z.; Verpoort, F.; Xiao, S. Taking the Place of Perylene Diimide: Perylene Tetracarboxylic Tetraester as a Building Block for Polymeric Acceptors to Achieve Higher Open Circuit Voltage in All-Polymer Bulk Heterojunction Solar Cells. *Polym. Chem.* **2013**, *4*, 5612−5620. (b) Seguy, I.; Jolinat, P.; Destruel, P.; Farenc, J.; Mamy, R.; Bock, H.; Ip, J.; Nguyen, T. P. Red Organic Light Emitting Device Made from Triphenylene Hexaester and Perylene Tetraester. *J. Appl. Phys.* **2001**, *89*, 5442−5448. (c) Gupta, R. K.; Ulla, H.; Satyanarayan, M. N.; Sudhakar, A. A. A Perylene-Triazine-Based Star-Shaped Green Light Emitter for Organic Light Emitting Diodes. *Eur. J. Org. Chem.* **2018**, *2018*, 1608−1613. (d) Bhargava, S.; Chu, J. J. H.; Valiyaveettil, S. Controlled Dye Aggregation in Sodium Dodecylsulfate-Stabilized Poly(methylmethacrylate) Nanoparticles as Fluorescent Imaging Probes. *ACS Omega* **2018**, *3*, 7663−7672.
(29) Haynes, W. M. *CRC Handbook of Chemistry and Physics: a Ready-reference Book of Chemical and Physical Data*, 96th ed.; CRC Press: Boca Raton, FL, 2015.
(30) Crosby, G. A.; Demas, J. N. Measurement of photoluminescence quantum yields. Review. *J. Phys. Chem.* **1971**, *75*, 991−1024.
(31) Langhals, H.; Karolin, J.; Johansson, L. B-A. Spectroscopic Properties of New and Convenient Standards for Measuring Fluorescence Quantum Yields. *J. Chem. Soc., Faraday Trans.* **1998**, *94*, 2919−2922.
(32) Lakowicz, J. R. *Principles of Fluorescence Spectroscopy*; Springer US: 2006.
(33) Berera, R.; van Grondelle, R.; Kennis, J. T. M. Ultrafast Transient Absorption Spectroscopy: Principles and Application to Photosynthetic Systems. *Photosynth. Res.* **2009**, *101*, 105−118.
(34) Snellenburg, J. J.; Laptenok, S.; Seger, R.; Mullen, K. M.; van Stokkum, I. H. M. Glotaran: A Java-Based Graphical User Interface for the R Package TIMP. *J. Stat. Soft.* **2012**, *49*, 22.
(35) van Stokkum, I. H. M.; Larsen, D. S.; van Grondelle, R. Global and Target Analysis of Time-resolved Spectra. *Biochim. Biophys. Acta, Bioenerg.* **2004**, *1657*, 82−104.
(36) Gorczak, N.; Renaud, N.; Tarkuc, S.; Houtepen, A. J.; Eelkema, R.; Siebbeles, L. D. A.; Grozema, F. C. Charge Transfer Versus Molecular Conductance: Molecular Orbital Symmetry Turns Quantum Interference Rules Upside Down. *Chem. Sci.* **2015**, *6*, 4196−4206.
(37) te Velde, G.; Bickelhaupt, F. M.; Baerends, E. J.; Fonseca Guerra, C.; van Gisbergen, S. J.; Snijders, J. G.; Ziegler, T. Chemistry with ADF. *J. Comput. Chem.* **2001**, *22*, 931−967.
(38) Weller, A. Photoinduced Electron Transfer in Solution: Exciplex and Radical Ion Pair Formation Free Enthalpies and their Solvent Dependence. *Z. Phys. Chem.* **1982**, *133*, 93.
(39) Goldsmith, R. H.; Sinks, L. E.; Kelley, R. F.; Betzen, L. J.; Liu, W.; Weiss, E. A.; Ratner, M. A.; Wasielewski, M. R. Wire-like Charge Transport at Near Constant Bridge Energy Through Fluorene Oligomers. *Proc. Natl. Acad. Sci. U. S. A.* **2005**, *102*, 3540−3545.
(40) Dubey, R. K.; Efimov, A.; Lemmetyinen, H. 1,7- And 1,6-Regioisomers of Diphenoxy and Dipyrrolidinyl Substituted Perylene Diimides: Synthesis, Separation, Characterization, and Comparison of Electrochemical and Optical Properties. *Chem. Mater.* **2011**, *23*, 778−788.
(41) Dubey, R. K.; Westerveld, N.; Sudholter, E. J. R.; Grozema, F. C.; Jager, W. F. Novel Derivatives of 1,6,7,12-tetrachloroperylene-3,4,9,10-tetracarboxylic acid: Synthesis, Electrochemical and Optical Properties. *Org. Chem. Front.* **2016**, *3*, 1481−1492.
(42) Inan, D.; Dubey, R. K.; Westerveld, N.; Bleeker, J.; Jager, W. F.; Grozema, F. C. Substitution Effects on the Photoinduced Charge-Transfer Properties of Novel Perylene-3,4,9,10-tetracarboxylic Acid Derivatives. *J. Phys. Chem. A* **2017**, *121*, 4633−4644.
(43) In order to cover a larger part of the solar spectrum, while retaining the photophysical properties, these antenna molecules can be extended by larger rylenes. See, for example, ref 10.
(44) Dubey, R. K.; Knorr, G.; Westerveld, N.; Jager, W. F. Fluorescent PET Probes Based on Perylene-3,4,9,10-tetracarboxylic Tetraesters. *Org. Biomol. Chem.* **2016**, *14*, 1564−1568.
(45) Dubey, R. K.; Niemi, M.; Kaunisto, K.; Efimov, A.; Tkachenko, N. V.; Lemmetyinen, H. Direct Evidence of Significantly Different Chemical Behavior and Excited-State Dynamics of 1,7- and 1,6-Regioisomers of Pyrrolidinyl-Substituted Perylene Diimide. *Chem. - Eur. J.* **2013**, *19*, 6791−6806.
(46) Hippius, C.; van Stokkum, I. H. M.; Zangrando, E.; Williams, R. M.; Würthner, F. Excited State Interactions in Calix[4]arene−Perylene Bisimide Dye Conjugates: Global and Target Analysis of Supramolecular Building Blocks. *J. Phys. Chem. C* **2007**, *111*, 13988−13996.
(47) Fron, E.; Schweitzer, G.; Osswald, P.; Würthner, F.; Marsal, P.; Beljonne, D.; Müllen, K.; De Schryver, F. C.; Van der Auweraer, M. Photophysical Study of Bay Substituted Perylenediimides. *Photochem. Photobiol. Sci.* **2008**, *7*, 1509−1521.
(48) Ford, W. E.; Hiratsuka, H.; Kamat, P. V. Photochemistry of 3,4,9,10-perylenetetracarboxylic dianhydride dyes. 4. Spectroscopic and Redox Properties of Oxidized and Reduced Forms of the bis(2,5-di-tert-butylphenyl)imide Derivative. *J. Phys. Chem.* **1989**, *93*, 6692−6696.
(49) In order to preserve the physical properties of the light harvesting molecules in devices, aggregation of the PTCA chromophores should be prevented, for example, by incorporation of these antenna molecules in organic frameworks.
(50) Pagoaga, B.; Mongin, O.; Caselli, M.; Vanossi, D.; Momicchioli, F.; Blanchard-Desce, M.; Lemercier, G.; Hoffmann, N.; Ponterini, G. Optical and Photophysical Properties of Anisole- and Cyanobenzene-substituted Perylene Diimides. *Phys. Chem. Chem. Phys.* **2016**, *18*, 4924−4941.
(51) Dubey, R. K.; Westerveld, N.; Grozema, F. C.; Sudhölter, E. J. R.; Jager, W. F. Facile Synthesis of Pure 1,6,7,12-Tetrachloroperylene-3,4,9,10-tetracarboxy Bisanhydride and Bisimide. *Org. Lett.* **2015**, *17*, 1882−1885.
(52) Dubey, R. K.; Westerveld, N.; Eustace, S. J.; Sudhölter, E. J. R.; Grozema, F. C.; Jager, W. F. Synthesis of Perylene-3,4,9,10-tetracarboxylic Acid Derivatives Bearing Four Different Substituents at the Perylene Core. *Org. Lett.* **2016**, *18*, 5648−5651.

DOI: 10.1021/acs.jpcc.8b08503
J. Phys. Chem. C 2019, 123, 36−47